Electron Oscillations in the Induced Martian Magnetosphere

J. D. Winningham, R.A. Frahm, J. R. Sharber, [a] A. J. Coates, D. R. Linder, Y. Soobiah [b], E. Kallio, [c] J.R. Espley [d] R. Lundin, S. Barabash, M. Holmström, H. Andersson, M. Yamauchi, A. Grigoriev, [e] J. R. Scherrer, S. J. Jeffers, [a] D. O. Kataria, [b] J. U. Kozyra,[f] J. G. Luhmann, [g] E. C. Roelof, D. J. Williams, S. Livi, [h] C. C. Curtis, K.C. Hsieh, B. R. Sandel, [i] H. Koskinen, [j] T. Säles, P. Riihela, W. Schmidt, [c] M. Grande, M. Carter, [k] J.-A. Sauvaud, A. Fedorov, J.-J. Thocaven, [l] S. McKenna-Lawler, [m] S. Orsini, R. Cerulli-Irelli, M. Maggi, [n] P. Wurz, P. Bochsler, [o] N. Krupp, J. Woch, M. Fraenz, [p] K. Asamura, [q] and C. Dierker [r]

[a] Southwest Research Institute, San Antonio, TX 7228-0510, USA

[b] Mullard Space Science Laboratory, University College London, Surrey RH5 6NT, UK

[c] Finnish Meteorological Institute, Box 503, FIN-00101 Helsinki, Finland

[d] Department of Physics and Astronomy, Rice University, Houston, TX, 77005, USA

[e] Swedish Institute of Space Physics, Box 812, S-98 128, Kiruna, Sweden

[f] Space Physics Research Laboratory, University of Michigan, Ann Arbor, MI 48109-2143, USA

[g] Space Science Laboratory, University of California in Berkeley, Berkeley, CA 94720-7450, USA

[h] Applied Physics Laboratory, Johns Hopkins University, Laurel, MD 20723-6099, USA

[i] University of Arizona, Tucson, AZ 85721, USA

[j] University of Helsinki, Department of Physical Sciences, P. O. Box 64, FIN-00014 Helsinki, Finland

[k] Rutherford Appleton Laboratory, Chilton, Didcot, Oxfordshire OX11 0QX, UK

[l] Centre d'Etude Spatiale des Rayonnements, BP-4346, F-31028 Toulouse, France

[m] Space Technology Ireland, National University of Ireland, Maynooth, Co. Kildare, Ireland

[n] Instituto di Fisica dello Spazio Interplanetari, I-00133 Rome, Italy

[o] University of Bern, Physikalisches Institut, CH-3012 Bern, Switzerland

[p] Max-Planck-Institut für Aeronomie, D-37191 Katlenburg-Lindau, German

[q] Institute of Space and Astronautical Science, 3-1-1 Yoshinodai, Sagamichara, Japan

[r] Technical University of Braunschweig, Hans-Sommer-Strasse 66, D-38106 Braunschweig, Germany

Pages: 38

Figures: 13

Proposed Running Head: Electron Oscillations in the Induced Martian Magnetosphere

Editorial correspondence to:

Dr. J.D. Winningham

Southwest Research Institute

PO Drawer 28510

6220 Culebra Road

San Antonio, TX 78228

Phone: 210-522-3075

Fax: 210-647-4325

E-mail address: dwinningham@swri.org

Abstract

The Analyzer of Space Plasmas and Energetic Atoms (ASPERA-3) experiment flown on the Mars Express (MEX) spacecraft includes the Electron Spectrometer (ELS) as part of its complement. The ELS instrument measures the differential electron flux spectrum in a 128-level logarithmic energy sweep within a time period of 4 sec. The orbital path of MEX traverses the Martian sheath, cusps, and tail where ELS recorded periodic electron intensity oscillations. These oscillations comprised periodic variations of up to an order of magnitude (peak to valley) in energy flux, with the largest amplitudes in the tens of eV to ~ 100s eV range. The observed oscillations displayed periods ranging from minutes down to the instrument sweep resolution of four seconds. In the cases analyzed here, the frequency of the integrated electron energy flux typically peaked between 0.01 and 0.02 Hz. This frequency range is nearly the same as the typical O^+ gyrofrequency in the magnetosheath, calculated using magnetometer data from Mars Global Surveyor. Due to the motion of the spacecraft, it is unclear if the wave structures observed were permanent standing waves or rather constituted waves propagating past the spacecraft.

Key Words: Oscillations, Mars Magnetosphere, Electrons, Electron Observations

1. Introduction

Espley et al. (2004) reported low frequency oscillations in the Martian Magnetosheath, Magnetic Pileup Region (MPR), and tail. Based on an extensive survey of magnetometer (MAG) data from the Mars Global Surveyor (MGS) spacecraft, these authors found that the fluctuations in the day side magnetosheath were mainly compressional, elliptically polarized with wave vectors at large angles to the mean field and with dominant frequencies significantly below the local proton gyrofrequency. Using kinetic plasma wave theory populations (see reviews by Gary, 1993 and Krauss-Verban et al., 1994), the authors tentatively identified the waves as due to mirror mode instabilities. Other workers (e.g. Sauer et al., 1998) used Phobos-2 observations and bi-ion fluid theory to identify nonlinear magneto-acoustic waves downstream of the Martian bowshock. In the night side magnetosheath, Espley et al. found the waves to be mainly transverse elliptically polarized waves at somewhat higher frequencies. These waves have been interpreted as being due to ion/ion resonant instabilities arising from counterstreaming ion populations.

These results provide an impetus for analyzing similar observations recorded at Mars aboard the Mars Express (MEX) spacecraft. However, MEX carried no science or aspect magnetometer. MEX did carry an electron spectrometer (ELS) and an ion mass spectrometer (IMA) as part of the Analyzer of Space Plasmas and Energetic Atoms (ASPERA-3) experiment. The ELS measurement frequency (4 sec per spectrum) is sufficient to observe most of the low frequency regime covered by the MGS magnetometer. Results will be presented from ELS that again demonstrate the presence in the close Martian environment of electron oscillations. As with most wave structures observed by a spacecraft which is in motion, it is unclear if the wave

structures observed were permanent standing waves or rather constituted waves propagating past the spacecraft. However, this does not change the fact that electron oscillations were observed.

Mars possesses no intrinsic planetary magnetic field; however, it does display localized crustal fields at the surface of the planet. These magnetic fields are described by Connerney et al. (2001). The solar wind and its interplanetary magnetic field (IMF) interact with Mars to form an induced magnetic field around the planet which stands off the solar wind. The solar wind interaction produces a bow shock (BS) in front of the planet. The region where the solar wind plasma is diverted around the planet is called the Martian Magnetosheath (MS). The boundary between the MS and the ionosphere/tail/inner magnetosphere is defined by Lundin et al. (2004) using ion signatures from MEX to constitute the Induced Magnetosphere Boundary (IMB). The IMB is located at or very near the magnetic pile-up boundary (MPB) defined by MGS, the difference being that the MPB is defined using the magnetic field signature and the IMB is defined using the particle signature. At and below the IMB, the crustal fields of Mars exert a significant influence on the shape of the IMB and on the behavior of its contained plasma (Brain, et al., 2004).

2. Instrument

The MEX ELS is a spherical top hat, which samples electrons from a 4º x 360º wide FOV, divided into 16 sectors, where each sector is 22.5º wide. The ELS k-factor or energy sensitivity (7.23 ± 0.05 eV/volt) and resolution ($\Delta E/E = 0.083 \pm 0.003$) (Sablik, et al., 1990) are slightly sector dependent and were determined by laboratory measurements at 10 keV. Energy deviations of the k-factor and resolution were folded into an energy-dependent relative

microchannel plate (MCP) efficiency factor. This allowed the energy independent physical geometric factor to be determined (5.88×10^{-4} cm^2 sr). A more complete description can be found in Barabash et al. (2003). The 360º acceptance plane of the ELS FOV is coplanar with the spacecraft XZ plane which, during this period is parallel to the ecliptic (Chicarco et al., 2004).

ELS covers the energy range from 1 eV to 20 keV and incorporates a deflection power supply which has two ranges. The ELS deflection voltage ranges from 0 to 20.99 V in its low range and from 0 to 2800.0 V in its high range. The energy conversion is sector dependent, but is approximately 150 eV (20 keV) at its maximum low (high) range value. Each supply range has a control resolution of 4096 linear voltage values within its full range. Of the 8192 possible deflection voltage values, 128 are selected to comprise the ELS energy sweep, which occurs in 4 sec.

Currently the ASPERA-3 data processing unit (DPU) is programmed to telemeter instrument engineering data instead of science data in place of every 8^{th} electron spectrum. This causes a time gap in the ELS spectrum information which, in the case of the Fourier analysis herein, is filled by linear interpolation between the adjacent measurements.

3. Observations

On August 9, 2004 (2004/222), the Mars Express spacecraft (orbit 711) traveled almost perpendicular to the flow in the magnetosheath in the dawn (~06 hours) sector. In planetodetic (Duxbury, 1979; and Lieske, et al., 1977) coordinates it was at ~0º latitude. Figure 1 shows the orientation of the Mars Express orbit as it traveled away from periapsis through the MS, and into

the solar wind at about 21:00 UT. While in the sheath, ELS observed periodic oscillations in the electron energy intensity (differential energy flux in units of ergs/(cm^2 sr eV sec)).

[Figure 1]

An energy-time spectrogram showing the ELS measured electrons from sector 3 (pointing approximately perpendicular to the orbit direction in the sheath flow ram direction) is displayed in the top panel of Figure 2. This spectrogram was recorded during the transit of Mars Express across the MS. Before 20:59:00 UT, ELS observes inner magnetosphere electron plasma (characterized by energy peaks around 10 eV). From 20:59:00 UT until 21:24:30 UT ELS observed MS electrons which showed a characteristic energy of about 50 eV. The differential energy flux intensity of the electrons oscillated during the crossing of the sheath. After 21:24:39 UT, the characteristic energy again decreased as ELS enters the solar wind plasma.

The ASPERA-3 experiment also contains an Ion Mass Analyzer (IMA) (Barabash et al., 2004). The IMA is a three stage analyzer: a 16 step elevation analyzer to select a polar angle, a top hat to select one of 96 ion energies, and a magnetic deflection system to determine mass from a 32 element anode. IMA cycles through its 96 energy steps and 16 elevation steps in 192 sec to create an energy-mass-azimuth-elevation measurement set. This 192 sec cycle time of IMA is too long when compared to the period of the electron oscillations observed in Figure 2. Thus, ion oscillations at the frequencies discussed in this paper could not be observed at this time.

[Figure 2]

A line plot of the differential electron energy flux integrated over energy for sensor 3 is included in the bottom panel (red curve) to emphasize the very regular nature of the electron oscillations recorded. Such pulsations are routinely observed by the MEX ELS. Statistical results will be presented in a later paper. The peak to valley ratio of the pulsations is about a factor of 10 (i.e., quite significant). Orbital parameters are provided at the bottom of the figure. In the middle panel a frequency time spectrogram of the power spectrum of the oscillations is provided. The power spectrum was created using a sliding Fourier Transform Technique (Hamming, 1962; Blackman and Tukey, 1958; Bevington, 1969; and Reiff, 1983) on the integrated differential energy flux. Very clear lines (~ 10 and 20 mHz) are seen in the f-t spectrograms, which show an orbital variation in both frequency and amplitude. In this analysis, a 5 minute wide window (150 spectra) was used which was consecutively slid forward by 4 seconds (1 spectrum at a time). The white gap is due to a lag of 5 minutes prior to the first calculated spectrum plotted. In the bottom panel the blue curve is the integrated wave power above 4 mHz. One can see the change in power as the spacecraft transited the sheath from the inside to the outside.

The power spectrum has been examined in more detail by means of the frequency spectral plots shown in Figure 3 which were recorded while traversing the sheath. These show that different frequency components tend to dominate at different locations within the MS. Figure 3a from 2107 to 2112 UT shows the power spectrum near the induced magnetospheric boundary (IMB), which is the envelope of the induced Martian magnetosphere (Lundin et al.,

2004). The horizontal line labeled LOS is the level of significance (Reiff, 1983) and represents the 2σ level. Peaks at frequencies of about 6.5 mHz and 12 mHz are observed. These frequencies are fairly constant until about 21:12:30 UT.

Toward the center of the MS, a disruption in the beating pattern took place. The frequency pattern (Figure 3b from 2110 to 2115 UT) shows the inclusion of high frequency peaks (with frequencies about 23 mHz, 35 mHz, and 47 mHz) and a reduction in amplitude at the lower frequencies. At the same time, the 12 mHz peak became more dominant in the power spectrum.

In the center of the MS (Figure 3c from 2113 to 2118UT, and Figure 3d from 2116 to 2121 UT), the lower frequency components vanished, and the amplitude and frequency patterns suggest that multiple harmonics of the 12 mHz signal are present. Toward the bow shock (Figure 3e from 2119 to 2124 UT), the higher frequency terms decayed in amplitude leaving behind the 12 mHz fundamental. Near the bow shock (Figure 3f from 2122 to 2127 UT), a peak at about 8 mHz appears; however, the peak at 12 mHz remained the larger.

[Figures 3a, 3b, 3c, 3d, 3e, 3f]

Figure 4 shows the projected orbit for February 5, 2005 (2005/036, orbit 1354). The electron data can be seen to be collected near noon (11 to 14 hours solar or local time) as the spacecraft passed from north to south of the planetodetic (PD) equator. At ~2110 UT MEX crossed the IMB into the MS and entered the solar wind at ~2150 UT. The electron data for the

sheath region during this pass is displayed in Figure 5. In the top panel of Figure 5 the same plasma oscillations are again seen, although they are more complex than in the earlier example. In general, this pass covered lower altitudes (450 to 3000 km as opposed to 2600 to 4800 km) with a smaller solar zenith angle (SZA) (less than 60º as opposed to 80º to 95º) than in the earlier example.

Viewing the data in Figure 5 from the direction of the solar wind interacting with the planet (right to left in Figure 5), one sees the amplitude of the oscillations building up as MEX crossed the bow shock (BS) from 2150 to 2142 UT. As the spacecraft then passed from the BS through the sheath and to the IMB, panels 2 and 3 of Figure 5 show a very dynamic frequency spectrum whose power and frequency peaks significantly vary. In general, the power decreases from the BS to the IMB as was also seen in the earlier case. As the spacecraft moved inward from the BS to the mid-sheath, higher frequency harmonics appeared and the power decreased. In this inner sheath region, one sees frequency peaks at ~10 to 20 mHz. By 2133 UT, in mid-sheath, a strong peak at 6 mHz is observed along with many harmonics up to 100 mHz. As the IMB was approached from the mid-sheath, the higher order harmonics diminished and the power dropped. (See the integrated power in the blue curve in the bottom panel.)

[Figure 4]

[Figure 5]

Next we examine the dusk to nightside region which was traversed on March 1, 2004 (2004/061, orbit 162) from 8 to 11 UT, see Figure 6. At approximately 0830 UT (13h local time) MEX entered the sheath region from the ionosphere at ~700 km. Throughout the remainder of the plot, MEX was located between the nominal Martian bow shock and the IMB (see Figure 7). MEX traversed the dusk sector at ~0915 UT, ~58º PD lat, and 6000 km altitude. From there it moved towards the equator and 22h local time near periapsis. As in the previous two examples, the record shows significant wave activity featuring multiple peaks. The power decreased progressively from noon to dusk to near midnight in the MS (see the blue curve in panel 3). Based on the three passes discussed, significant ULF power was a characteristic feature from dawn to noon to dusk and up to mid-Martian latitudes.

[Figure 6]

[Figure 7]

Heated, pulsating electrons were also recorded inside the Martian magnetotail. An example is shown in Figure 8 covering the interval 0100 to 0141 UT May 20, 2004 (2004/141, orbit 419). From the beginning of these observations MEX was within the shadow of Mars (See Figure 9). Up to ~0112 UT, UV radiation from the distant Martian UV limb created spacecraft photoelectrons. A population of heated electrons endured beyond this time up until ~0128 UT. Dramatic oscillations are seen in the particle data in the top panel. In the middle panel a clear peak develops at ~16 mHz, with associated high harmonics. At ~0125 UT a peak at about 5 mHz appears and the power also jumps up (see bottom panel blue curve). The oscillations end at

~0130 UT. This case provides an observation of "nightside" oscillations with interesting implications for Martian magnetospheric topology. It is also possible that these observations could be due to tail flapping or surface waves. In this heated region no ions were observed.

[Figure 8]

[Figure 9]

We present in Figure 10 data from the pass immediately following the one discussed in the previous paragraph (orbit 420). A similar burst of oscillating, heated electrons is observed centered at ~0750 UT. Figure 11 shows that this pass was very similar to that of Figures 6 and 7 from about 0610 UT, where MEX exited the solar wind near apoapsis at ~19h local time and moved across the sheath towards the nightside. Once again the power decreased as MEX progressed crossstream. At approximately 0720 UT we see a burst in electron flux and wave power in the same frequency regime as that discussed earlier, near the nominal IMB. Beyond this boundary the electrons cooled until ~0738 UT where the heating increased until it peaked at ~0750 UT and faded by ~0801 UT. The heating recorded at the maximum was quite variable. Possible physical reasons for this will be explored in future papers. Again, this was approximately the time when scattered UV from the Martian limb was no longer present. Typical ULF spectral peaks were observed. In this example, ions were identified to be present during the heating event.

[Figure 10]

[Figure 11]

Now we turn to the dayside below the IMB. As seen in Figure 12 the spacecraft at just past noon was near periapsis at the planetodetic equator on January 9, 2005 (2005/009, orbit 1257). From ~1712 to 1716 UT heated oscillating electrons were recorded (Figure 13). In addition, ions were concurrently observed, as in the case of the second nightside heated population discussed above. Plasma oscillations in the same ULF frequency regime are seen in the middle panel. The power is much less (see bottom panel) than in the MS from ~1722 UT onward. This sheath is in the morning, southern region. Soobiah et al., (this issue) presented observations consistent with Martian "magnetic cusps" resulting from the vertical component of the remnant field. In this event the observations were not made over one of these remnant features but they show the same ion and electron signatures characteristic of direct MS plasma access.

[Figure 12]

[Figure 13]

We also report evidence in ELS data for ULF plasma waves in the Martian MS, tail and cusps (similar to the MGS MAG results), over a range of local times, latitudes, and regions. These features were found to be present in essentially all of these regions based on the present random sampling. In a later paper we will present a statistical study of this material.

4. Discussion

Periodic fluctuations of electron fluxes were observed in the magnetosheath, magnetotail and magnetic "cusps" of Mars. They were observed on both the dawn and dusk sides of Mars as well as above and below the planetodetic equator. A Fourier analysis was performed on the integral of the electron flux. The resulting power spectra demonstrated that there was significant power in the ULF range, in conformity with the report of the MGS magnetometer team (Espley et al., 2004). Detailed examination of the power spectra revealed peaks from 5 mHz (the lower frequency limit is ~ 4 mHz) upwards. At times, fundamentals and harmonic tones were clearly visible in the spectra. Peaks in the spectra showed a variation when samples were taken at different positions with respect to Mars. Based on the limited data set presented, the wave power maximizes in the vicinity of the bow shock and decreases progressively downstream from the shock. Interestingly, similar results were obtained on the dayside in regions where Martian magnetic cusps are formed due to the interaction of the remanent crustal fields with the solar wind magnetic field. This result is not surprising since one expects a direct connection with the sheath population via these magnetic cusps features. The presence of similar power spectra in the sheath and cusps points to the intimate interconnection of these regions.

A little more surprising is the observation of similar fluctuations in regions of electron bursts inside the Martian magnetotail. In both the cusp and tail events ions were also observed, but not over 100% of the time (See Lundin et al, this issue). We have presented in this paper one event with and one without ions, separated in time by one orbit. The spectral peaks and power levels in these events are similar to those observed in the MS region. This raises the intriguing

possibility of a direct connection between these regions. A likely mechanism would be the extension of the crustal field to large distances behind Mars near the magnetotail boundary. A later paper will explore the regions of occurrence of these electron bursts. A preliminary look indicates that they cluster near the umbra of Mars.

In this data set, the predominant fundamental frequency is ~ 12 mHz. Unfortunately there is no magnetometer aboard MEX. Espley et al (2004) suggested that some of the frequencies they observed are close to the O^+ ion gyrofrequency. Oxygen and heavier ions have been observed by the ASPERA-3 Ion Mass Spectrometer in some of the passes presented herein as well as others (Lundin et al., 2004; Lundin et al, this issue). Recall also the report of the detection of copious quantities of O+ ions by the SLED instrument at Mars during the Phobos Mission (McKenna-Lawlor et al., 1998). If we use O^+ and 12 mHz the total magnetic field of 20 nT can be inferred, which is a reasonable value. The variation in the fundamental frequency could be due to changing composition and magnetic field values around Mars. In general, this is consistent with the work of Espley et al. (2004) and could be indicative of bunches of planetary ions gyrating out from the planet in resonance with the solar wind.

As mentioned earlier, the ion spectrometer cannot resolve these fluctuations. However, for scale lengths greater than the Debye length, the plasma should be electrically neutral. Therefore, when relatively large scale, relatively slow ion wave modes develop, they carry with them (on these large scales) the electrons that are associated with the oscillating ions. The electrons of course experience their own wave behavior, but at much higher frequencies and at

much shorter wave lengths. When observed at ULF time scales, the electrons trace the motions of the ions and the ion wave modes.

Based on the MGS magnetic observations and the electron results of MEX one can speculate on the physical processes involved in generating these waves. For example, it is possible that between the magnetic field and the plasma the total particle and magnetic pressures remain constant, although there is an interchange of energy. Similar results have been observed at earth. Many other instabilities are possible as pointed out by Espley et al (2004). Later papers will investigate these various possibilities in more detail.

5. Summary

The MEX ASPERA ELS experiment has clearly shown ULF fluctuations to be very common around Mars. Our preliminary observations indicate that the bow shock may be the source of the oscillations, but also the whole magnetosheath and nightside are responding. Their power spectra are similar to those observed by MGS MAG, pointing to a common physical source. These fluctuations also point to the possibility of the effects of the Martian remanent field extending to great distances from Mars and interconnecting with the solar wind field on both the day and the nightside of Mars. The results also point to the presence of heavy ions ($>O^+$) around Mars. One can conclude that Mars is far from a passive environment despite its lack of a large permanent magnetic field.

Acknowledgement

The ASPERA-3 experiment on the European Space Agency (ESA) Mars Express mission is a joint effort between 15 laboratories in 10 countries, all sponsored by their national agencies. We thank all these agencies as well as the various departments/institutes hosting these efforts. We wish to acknowledge support of NASA contract NASW00003 for the support of the design, construction, operation, and data analysis for the Electron Spectrometer through the Discovery Program Mission of Opportunity.

We also wish to acknowledge the Swedish National Space Board for their support of the main PI-institute and we are indebted to ESA for their courage in embarking on the Mars Express program, the first ESA mission to the red planet.

References

Barabash, S., 46 colleagues, 2004. ASPERA-3: Analyser of Space Plasmas and Energetic Ions for Mars Express, in MARS EXPRESS: The Scientific Payload, ed. A. Wilson, European Space Agency Publications Division, European Space Research & Technology Centre, Noordwijk, The Netherlands, SP-1240, pp. 121-139.

Bevington, P.R., 1969. Data Reduction and Error Analysis for the Physical Sciences, McGraw-Hill: New York.

Blackman, R.B. Tukey, J.W., 1958. The Measurement of Power Spectra From the Point of View of Communication Engineering, Dover: New York.

Brain, D.A., Bagenal, F., Acuña, M.H., Connerney, J.E.P., 2003. Martian Magnetic Morphology: Contributions from the Solar Wind and Crust, J. Geophys. Res., 108, A12, pp. SMP 8-1.

Chicarro, A., Martin, P., Trautner, R., 2004. The Mars Express Mission: An Overview in MARS EXPRESS: The Scientific Payload, ed. A. Wilson, European Space Agency Publications Division, European Space Research and Technology Centre, Noordwijk, The Netherlands, SP 1240, pp. 3-13.

Connerney, J.E.P., Acuña, M.H., Wasilewski, P.J., Kletetschka, G., Ness, N.F., Rème, H., Lin, R.P., Mitchell, D.L., 2001. The Global Magnetic Field of Mars and Implications for Crustal Evolution, Geophysical Research Letters, 28, Issue 21, 4015-4018, doi: 10.1029/2001GL013619.

Duxbury, T. C., 1979. Planetary Geodetic Control Using Satellite Imaging, Journal of Geophysical Research, 84, pp. 1125-1128.

Espley, J.R., Cloutier, P.A., Brain, D.A., Crider, D.H., Acuña, M.H., 2004. Observations of Low-Frequency Magnetic Oscillations in the Martian Magnetosheath, Magnetic Pileup Region, and Tail, J. Geophys. Res., 109, A07213-A07213, doi: 10.1029/2003JA010193.

Gary, S.P., 1993. Theory of Space Plasma Microinstabilities, Cambridge Univ. Press, New York.

Hamming, R.W., 1962. Numerical Methods for Scientists and Engineers, McGraw-Hill: New York.

Krauss-Varban, D., Omidi, N., Quest, K.B., 1994. Mode Properties of Low-Frequency Waves: Kinetic Theory Versus Hall-MHD, J. Geophys. Res., 99, 5987-6009.

Lieske, J.H., Lederle, T., Fricke, W., Marando B., 1977. Expansions for the Precession Quantities Based upon the IAU (1976) System of Astronomical Constants, Astronomy and Astrophysics, 1-16.

Lundin, R., 43 colleagues, this issue. Ionospheric Plasma Acceleration at Mars: ASPERA-3 Results.

Lundin, R., 44 colleagues, 2004. Solar Wind-Induced Atmospheric Erosion at Mars: First Results from ASPERA-3 on Mars Express, Science, 305, pp. 1933-1936.

McKenna-Lawlor, S., Afonin, V.V., Kirsch, E., Schwingenschuh, K., Slavin, J.A., Trotignon, J.G., 1998. An Overview of Energetic Particles (from 55 keV to > 30 MeV) Recorded in the Close Martian Environment and their Energization in Local and External Processes, Planet. Space Sci., 46, pp. 83-102.

Sablik, M.J., Scherrer, J.R., Winningham, J.D., Frahm, R.A., Schrader, T., 1990. TFAS (A Tophat for all Species): Design and Computer Optimization of a New Electrostatic Analyzer, IEEE Transactions on Geoscience and Remote Sensing, 28, pp. 1034-1048.

Sauer, K., Dubinen, E., K. Baumgärtel, Tarasov, V., 1998. Low-Frequency Electromagnetic Waves and Instabilities within the Martian Bi-Ion Plasma, Earth Planets Space, 50, pp. 269-278.

Soobiah, Y., 42 colleagues, this issue. Observations of magnetic anomaly signatures in Mars Express ASPERA-3 ELS Data.

Reiff, P.H., 1983. The Use and Misuse of Statistical Analysis, in Solar-Terrestrial Physics: Theoretical Foundations, edited by R.L. Carovillano and J.M. Forbes, Reidel: Dordrecht, Holland.

Figure captions

Figure 1. Mars Express orbit 711 on August 9, 2004. The Mars Express spacecraft traveled from periapsis, through the sheath, and into the solar wind nearly perpendicular to the sheath flow. While in the sheath, ELS recorded oscillations in the electron plasma. This plot is in Mars cylindrical coordinates and the outer two blue curves represent the nominal bow shock and induced magnetospheric boundary.

Figure 2. Electron spectrogram (top panel) of electron oscillations for orbit 711, August 9, 2004. Shown are data from the ELS measurements of the energy intensity oscillations (upper panel). This energy intensity was Fourier analyzed and the resulting frequency spectrogram is shown in the center panel. The bottom panel shows the integrated energy flux (left annotation) and integrated power (right annotation) above the line of significance.

Figure 3. Selected frequency spectra throughout the sheath transit. Power spectra from the Fourier analysis are displayed at intervals of about every 3 minutes to cover the period when Mars Express crossed the sheath; a) near the inner magnetospheric boundary, b) toward the inner magnetospheric boundary, c) and d) at the center of the sheath, e) toward the bow shock, f) near the bow shock. Significant frequencies are greater than 4 mHz. Significant amplitudes are above the line of significance (LOS).

Figure 4. Same as Figure 1 for orbit 1354 on February 2, 2005.

Figure 5. Same as Figure 2 for orbit 1354 on February 2, 2005.

Figure 6. Same as Figure 2 for orbit 162 on March 1, 2004.

Figure 7. Same as Figure 1 for orbit 162 on Mary 1, 2004.

Figure 8. Same as Figure 2 for orbit 419 on May 20, 2004.

Figure 9. Same as Figure 1 for orbit 162 on May 20, 2004.

Figure 10. Same as Figure 2 for orbit 420 on May 20, 2004.

Figure 11. Same as Figure 1 for orbit 420 on May 20, 2004.

Figure 12. Same as Figure 2 for orbit 1257 on January 9, 2005

Figure 13. Same as Figure 1 for orbit 1257 on January 9, 2005

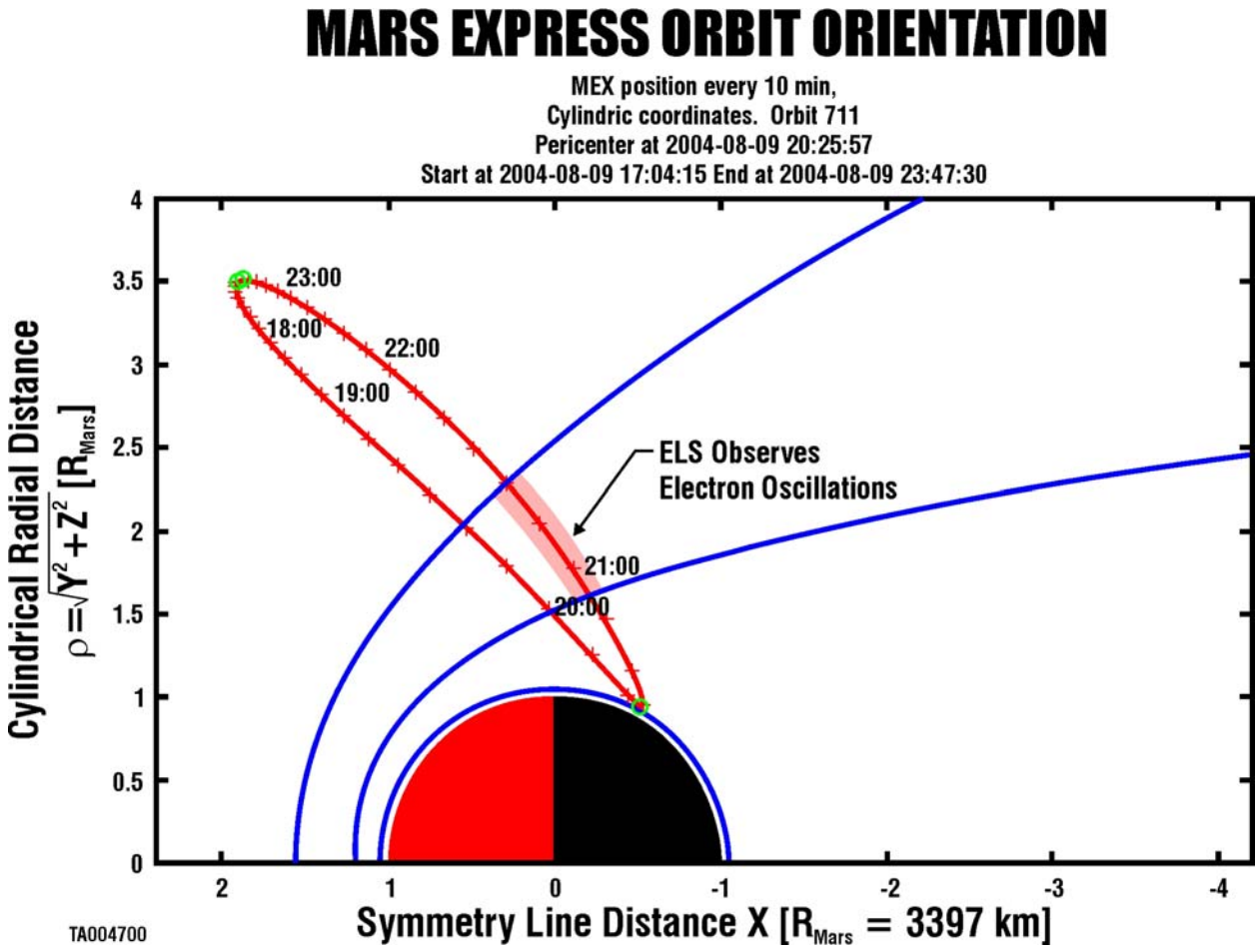
MARS EXPRESS ORBIT ORIENTATION
MEX position every 10 min,
Cylindric coordinates. Orbit 711
Pericenter at 2004-08-09 20:25:57
Start at 2004-08-09 17:04:15 End at 2004-08-09 23:47:30
23:00
18:00
22:00
19:00
ELS Observes
Electron Oscillations
21:00
20:00
Cylindrical Radial Distance
ρ=√(Y²+Z²) [R_Mars]
Symmetry Line Distance X [R_Mars = 3397 km]
TA004700

Figure 1

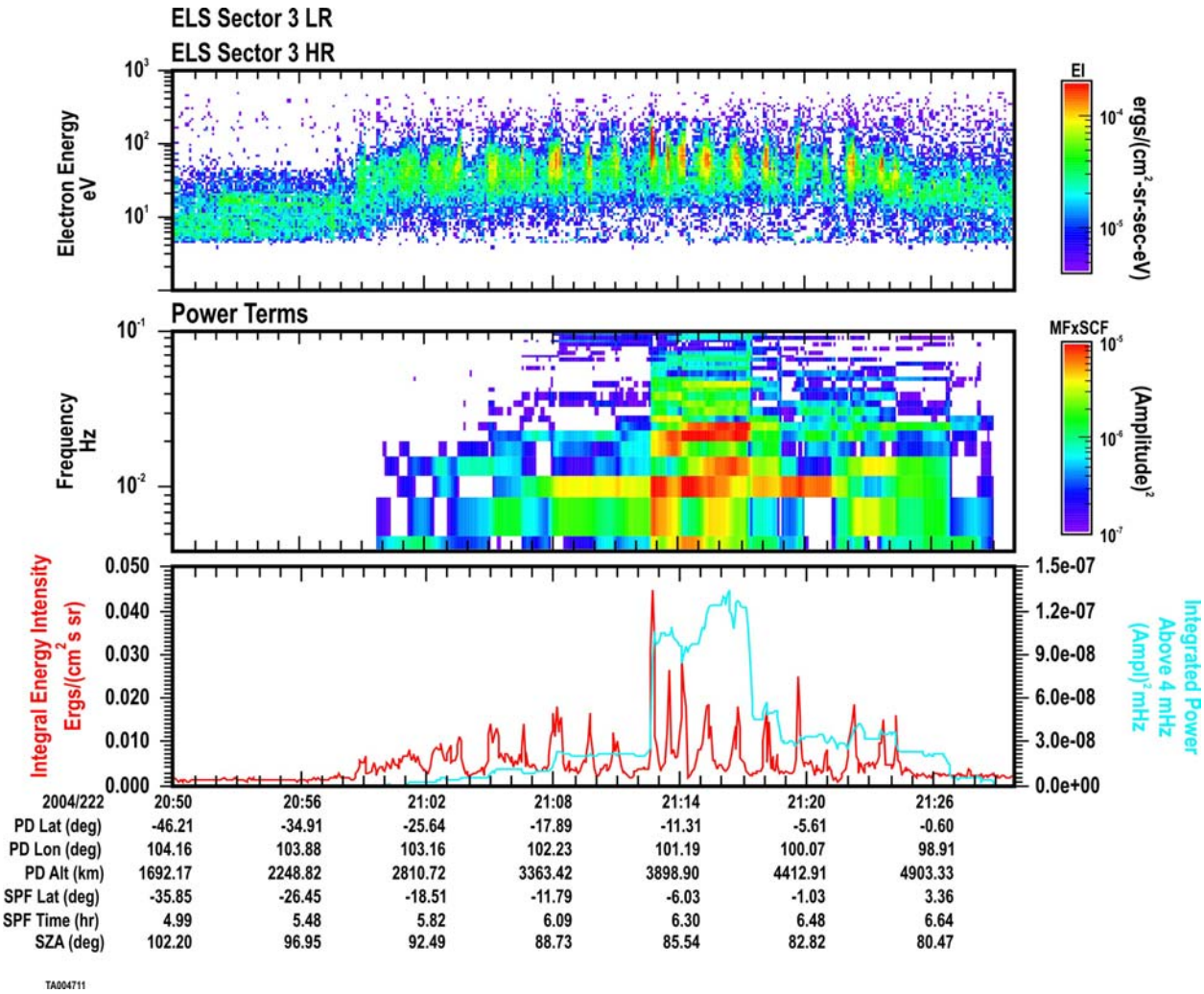
ELS Sector 3 LR
ELS Sector 3 HR
Electron Energy eV
EI
ergs/(cm²-sr-sec-eV)
Power Terms
Frequency Hz
MFxSCF
(Amplitude)²
Integral Energy Intensity Ergs/(cm² s sr)
Integrated Power Above 4 mHz (Ampl)² mHz
2004/222
PD Lat (deg)
PD Lon (deg)
PD Alt (km)
SPF Lat (deg)
SPF Time (hr)
SZA (deg)
20:50 20:56 21:02 21:08 21:14 21:20 21:26
-46.21 -34.91 -25.64 -17.89 -11.31 -5.61 -0.60
104.16 103.88 103.16 102.23 101.19 100.07 98.91
1692.17 2248.82 2810.72 3363.42 3898.90 4412.91 4903.33
-35.85 -26.45 -18.51 -11.79 -6.03 -1.03 3.36
4.99 5.48 5.82 6.09 6.30 6.48 6.64
102.20 96.95 92.49 88.73 85.54 82.82 80.47
TA004711

Figure 2

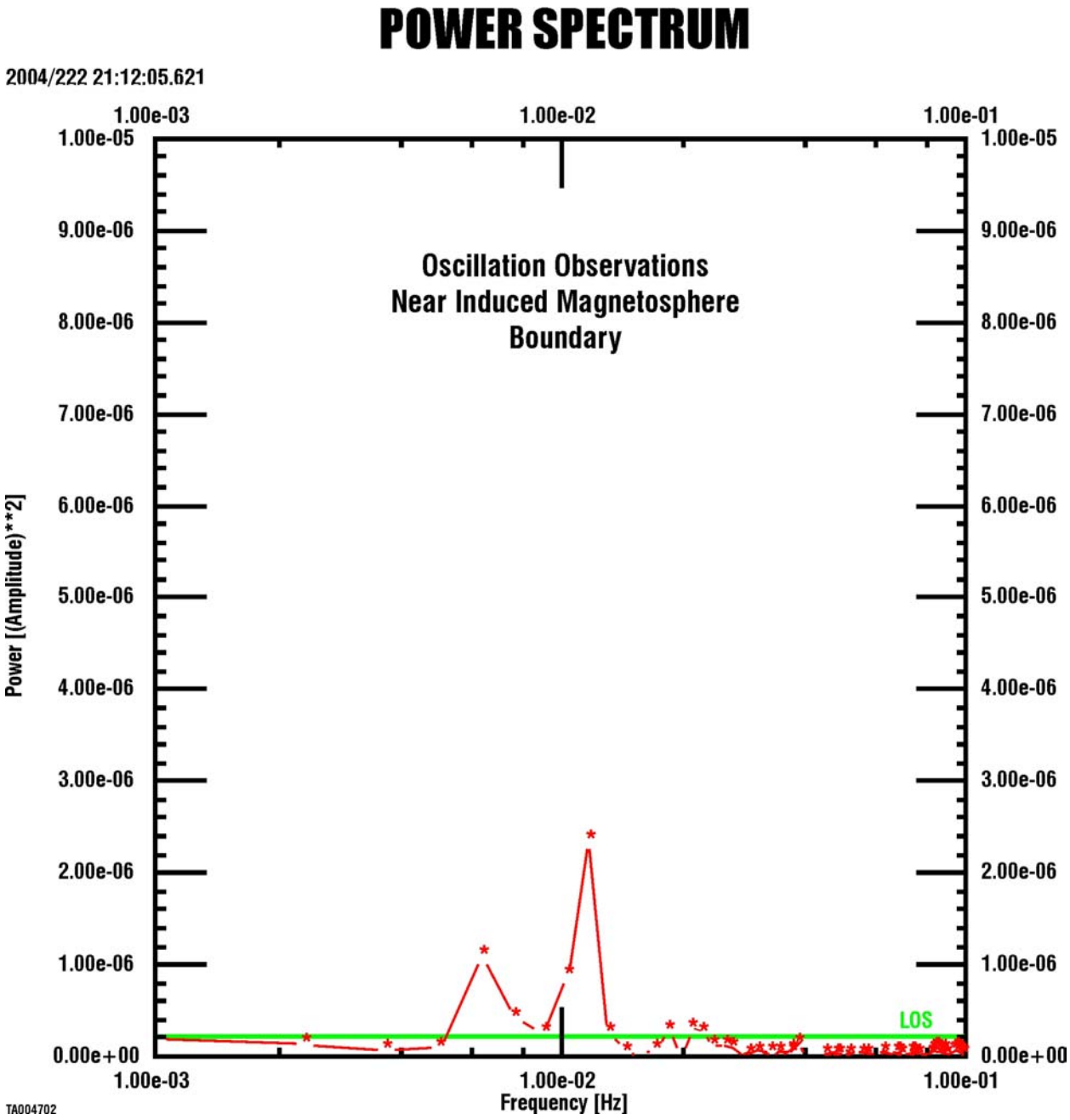
POWER SPECTRUM
2004/222 21:12:05.621
Oscillation Observations
Near Induced Magnetosphere
Boundary
LOS
Power [(Amplitude)**2]
Frequency [Hz]
1.00e-03
1.00e-02
1.00e-01
1.00e-05
9.00e-06
8.00e-06
7.00e-06
6.00e-06
5.00e-06
4.00e-06
3.00e-06
2.00e-06
1.00e-06
0.00e+00
TA004702

Figure3a

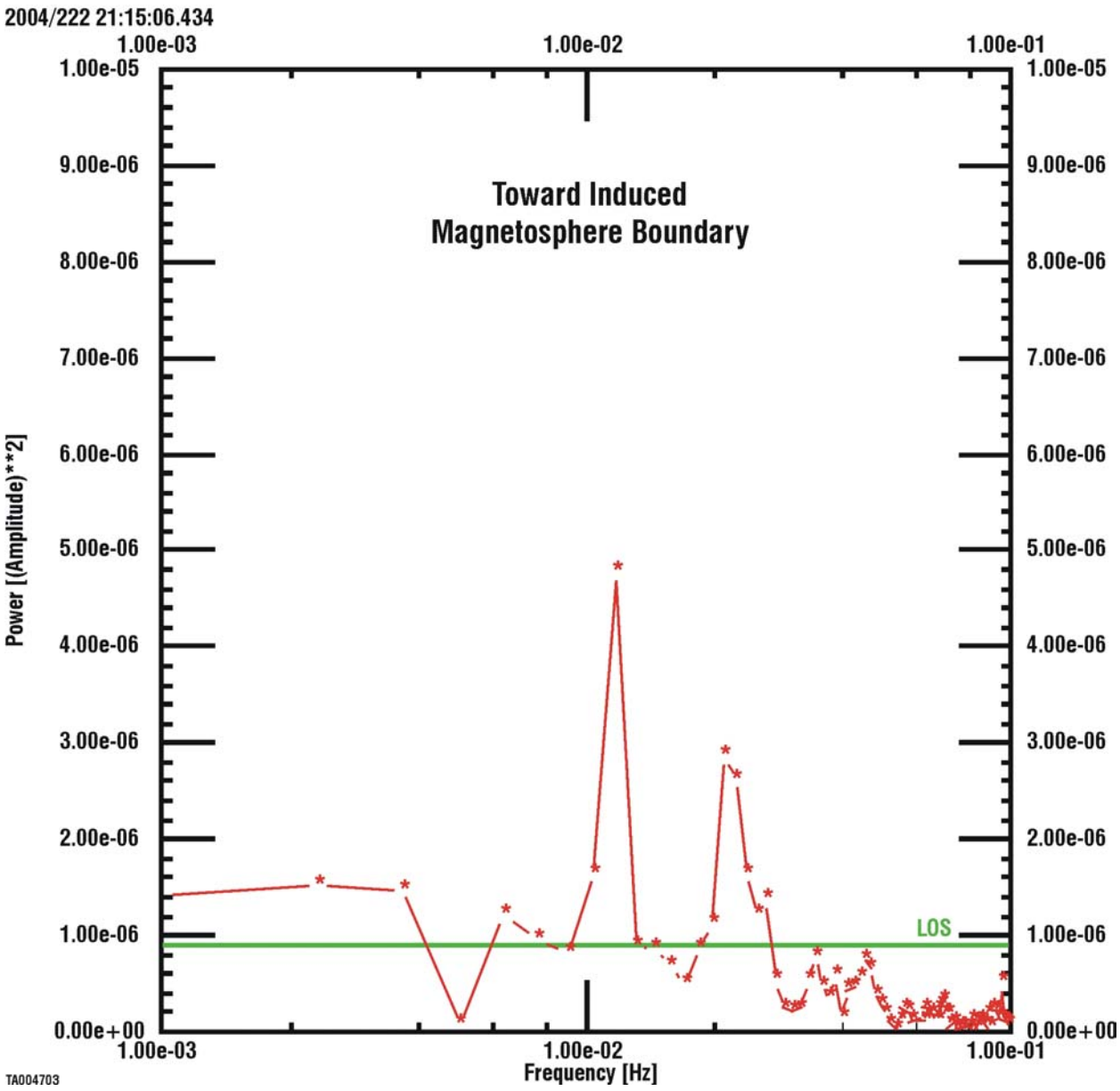
POWER SPECTRUM
2004/222 21:15:06.434
1.00e-03
1.00e-02
1.00e-01
1.00e-05
9.00e-06
8.00e-06
7.00e-06
6.00e-06
5.00e-06
4.00e-06
3.00e-06
2.00e-06
1.00e-06
0.00e+00
Toward Induced
Magnetosphere Boundary
LOS
Power [(Amplitude)**2]
Frequency [Hz]
TA004703

Figure 3b

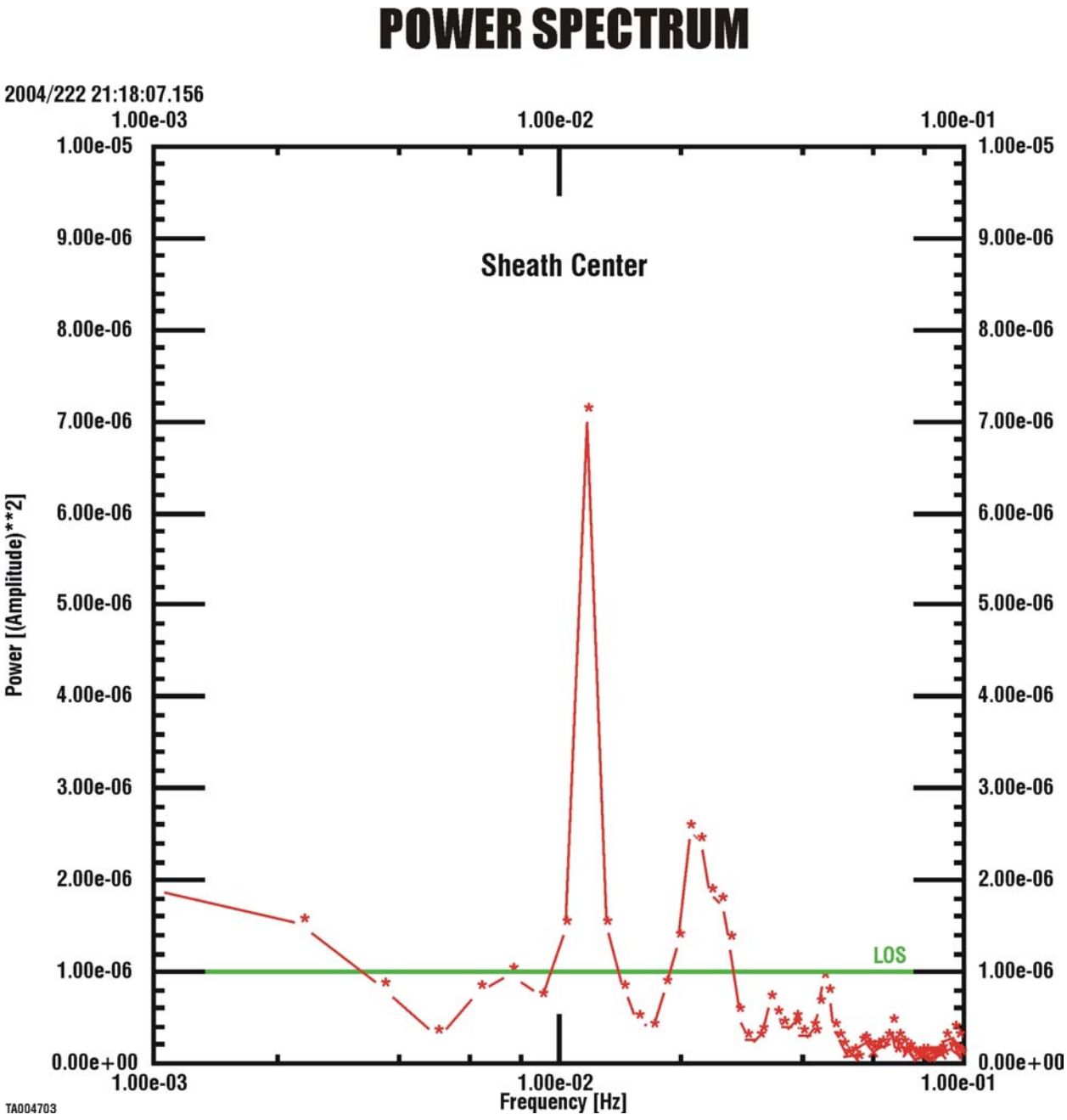
POWER SPECTRUM
2004/222 21:18:07.156
Sheath Center
LOS
Power [(Amplitude)**2]
Frequency [Hz]
1.00e-03
1.00e-02
1.00e-01
1.00e-05
9.00e-06
8.00e-06
7.00e-06
6.00e-06
5.00e-06
4.00e-06
3.00e-06
2.00e-06
1.00e-06
0.00e+00
TA004703

Figure 3c

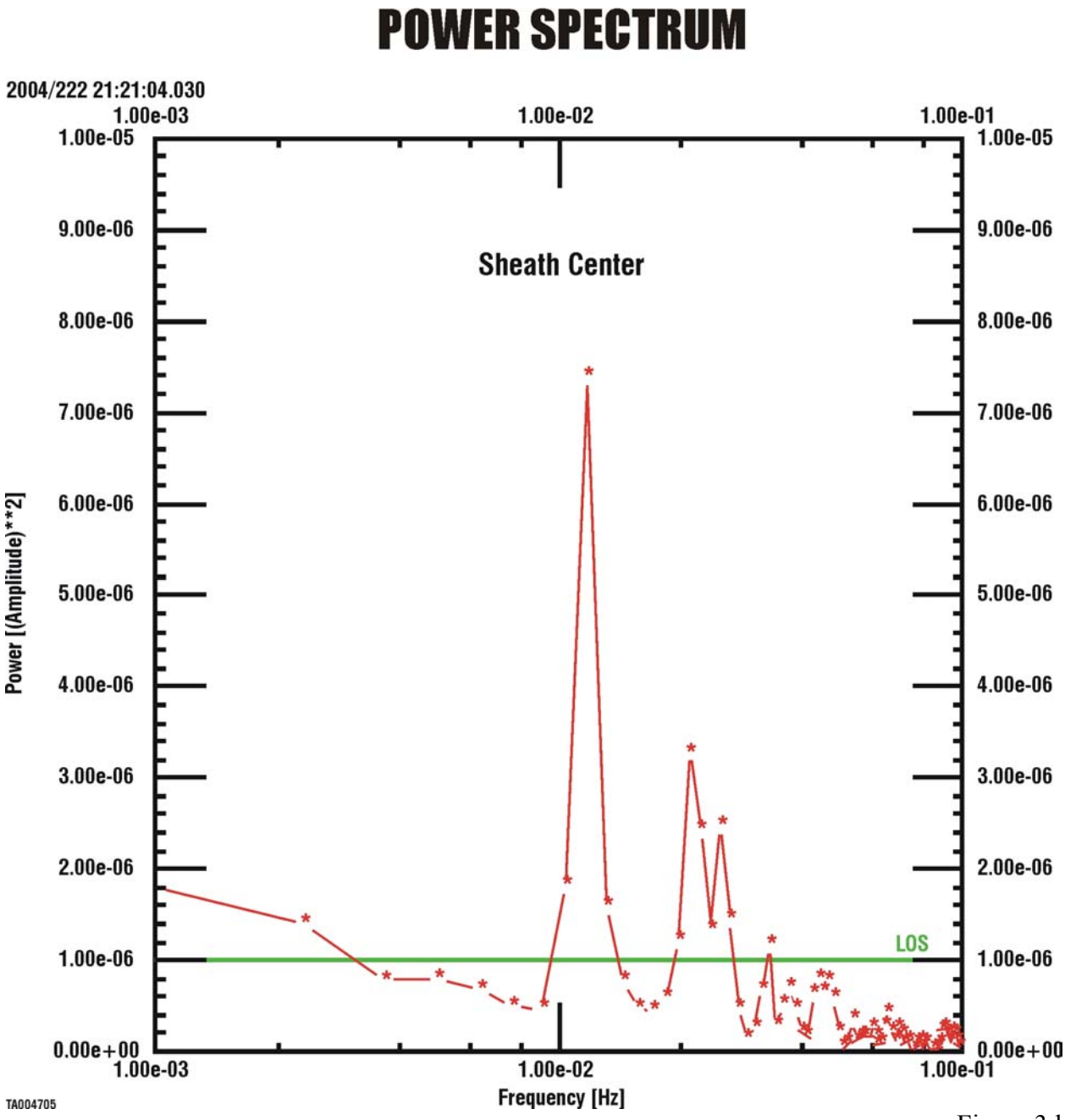
POWER SPECTRUM
2004/222 21:21:04.030
Sheath Center
LOS
Power [(Amplitude)**2]
Frequency [Hz]
1.00e-03
1.00e-02
1.00e-01
1.00e-05
9.00e-06
8.00e-06
7.00e-06
6.00e-06
5.00e-06
4.00e-06
3.00e-06
2.00e-06
1.00e-06
0.00e+00
TA004705

Figure 3d

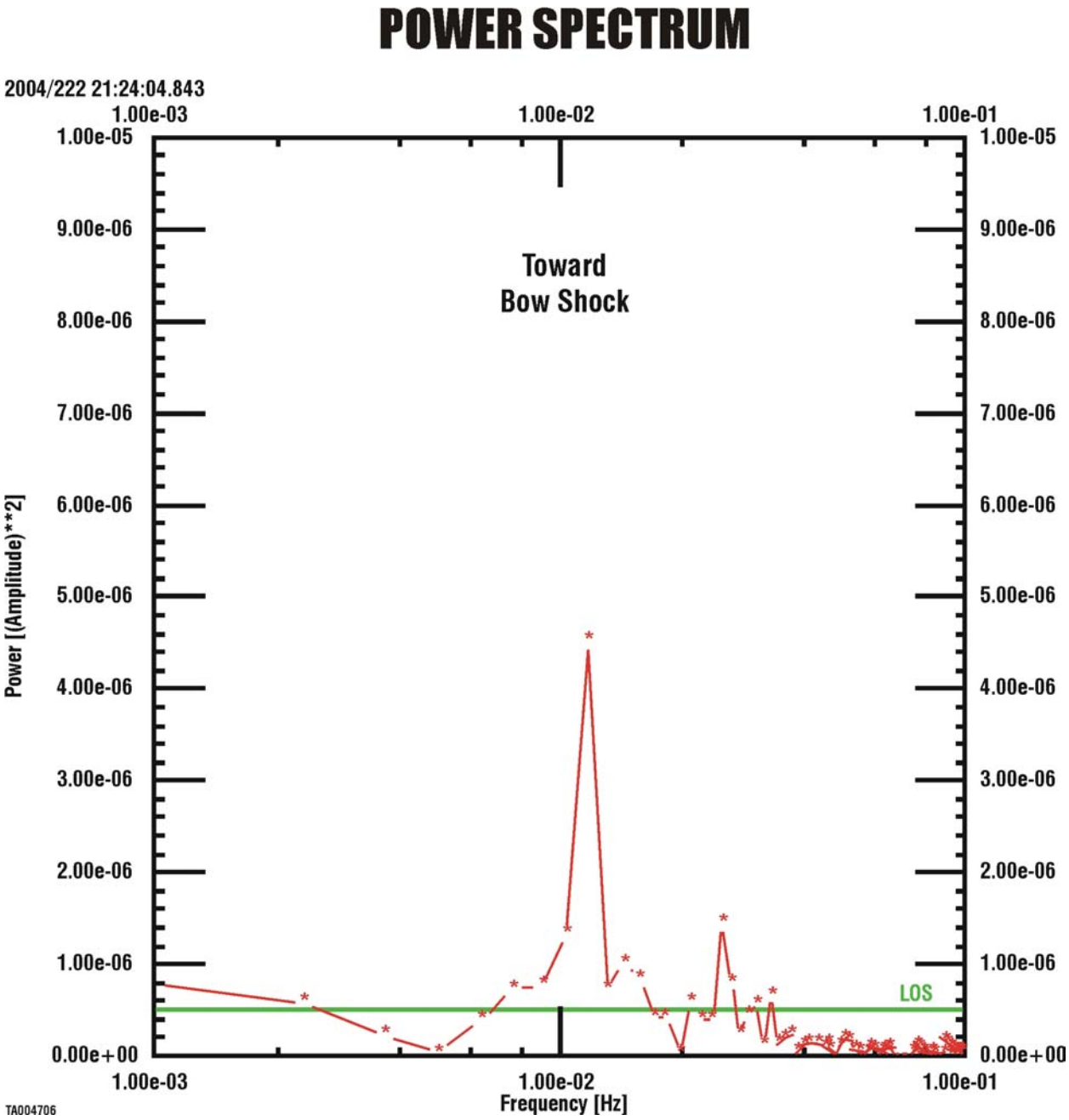
POWER SPECTRUM
2004/222 21:24:04.843
1.00e-03
1.00e-02
1.00e-01
1.00e-05
9.00e-06
8.00e-06
7.00e-06
6.00e-06
5.00e-06
4.00e-06
3.00e-06
2.00e-06
1.00e-06
0.00e+00
Toward
Bow Shock
LOS
Power [(Amplitude)**2]
Frequency [Hz]
TA004706

Figure 3e

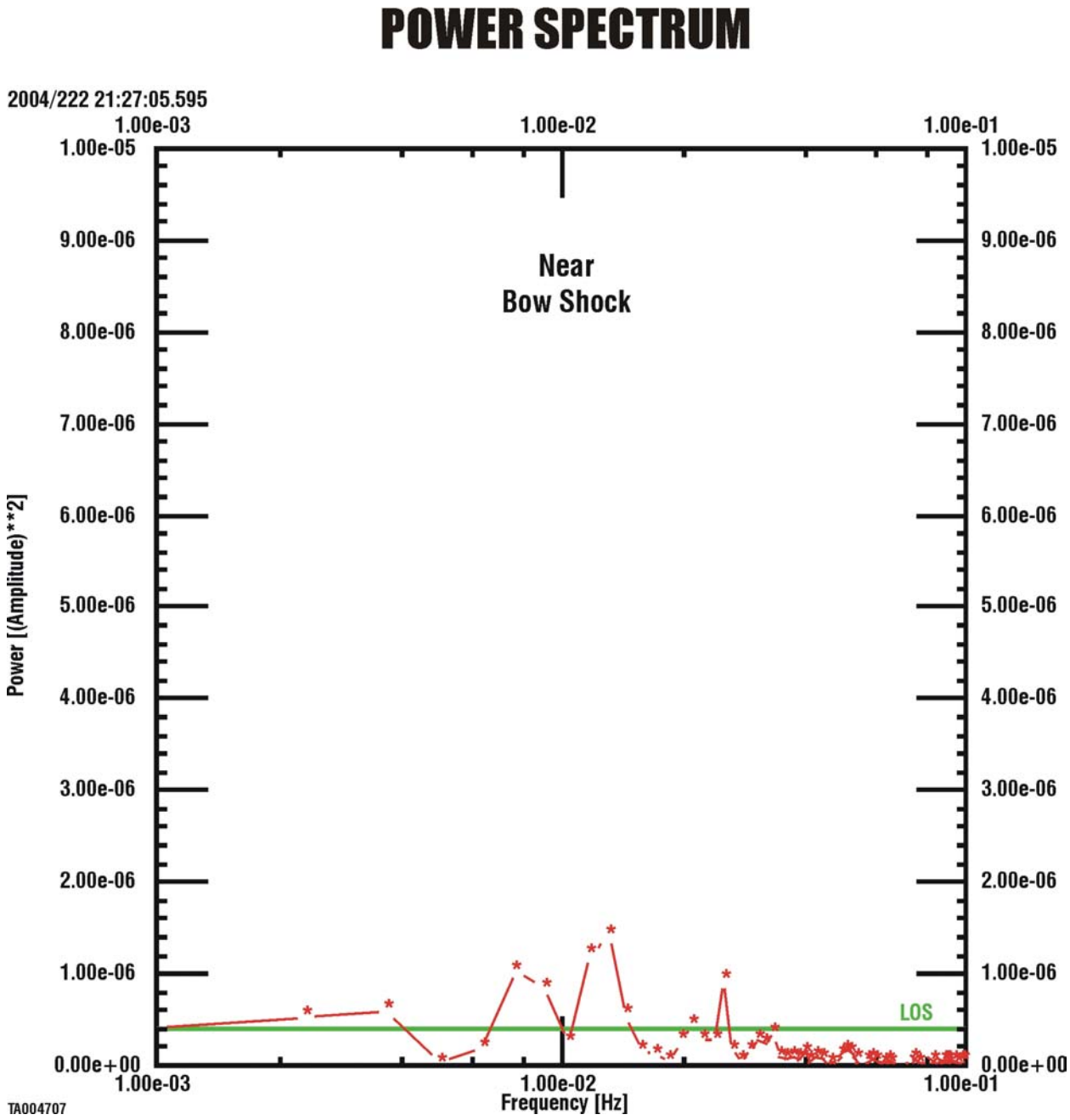
POWER SPECTRUM
2004/222 21:27:05.595
1.00e-03
1.00e-02
1.00e-01
1.00e-05
9.00e-06
8.00e-06
7.00e-06
6.00e-06
5.00e-06
4.00e-06
3.00e-06
2.00e-06
1.00e-06
0.00e+00
Near
Bow Shock
LOS
Power [(Amplitude)**2]
Frequency [Hz]
TA004707

Figure 3f

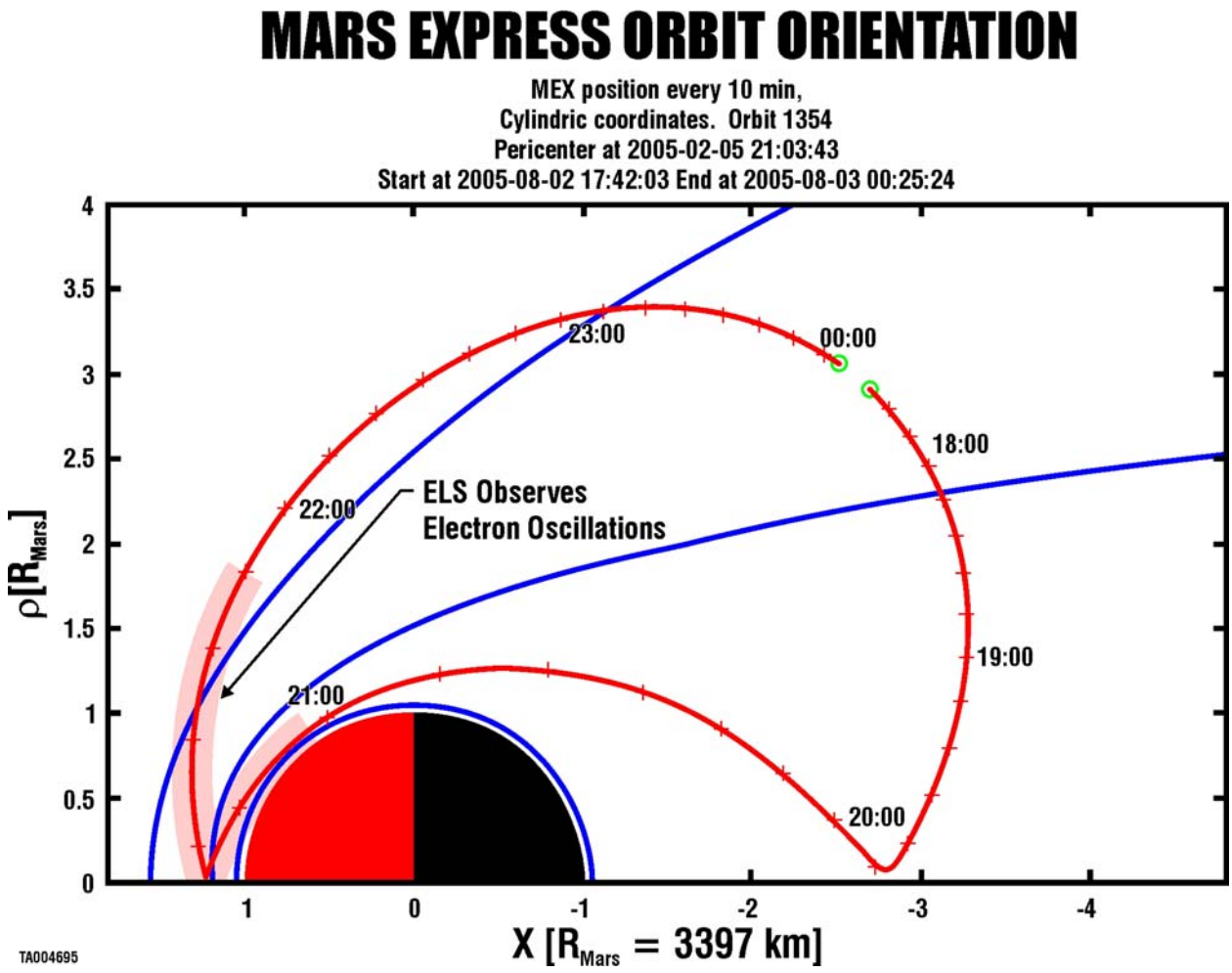
MARS EXPRESS ORBIT ORIENTATION
MEX position every 10 min,
Cylindric coordinates. Orbit 1354
Pericenter at 2005-02-05 21:03:43
Start at 2005-08-02 17:42:03 End at 2005-08-03 00:25:24
ELS Observes
Electron Oscillations
23:00
00:00
18:00
22:00
19:00
21:00
20:00
ρ[R_Mars]
X [R_Mars = 3397 km]
TA004695

Figure 4

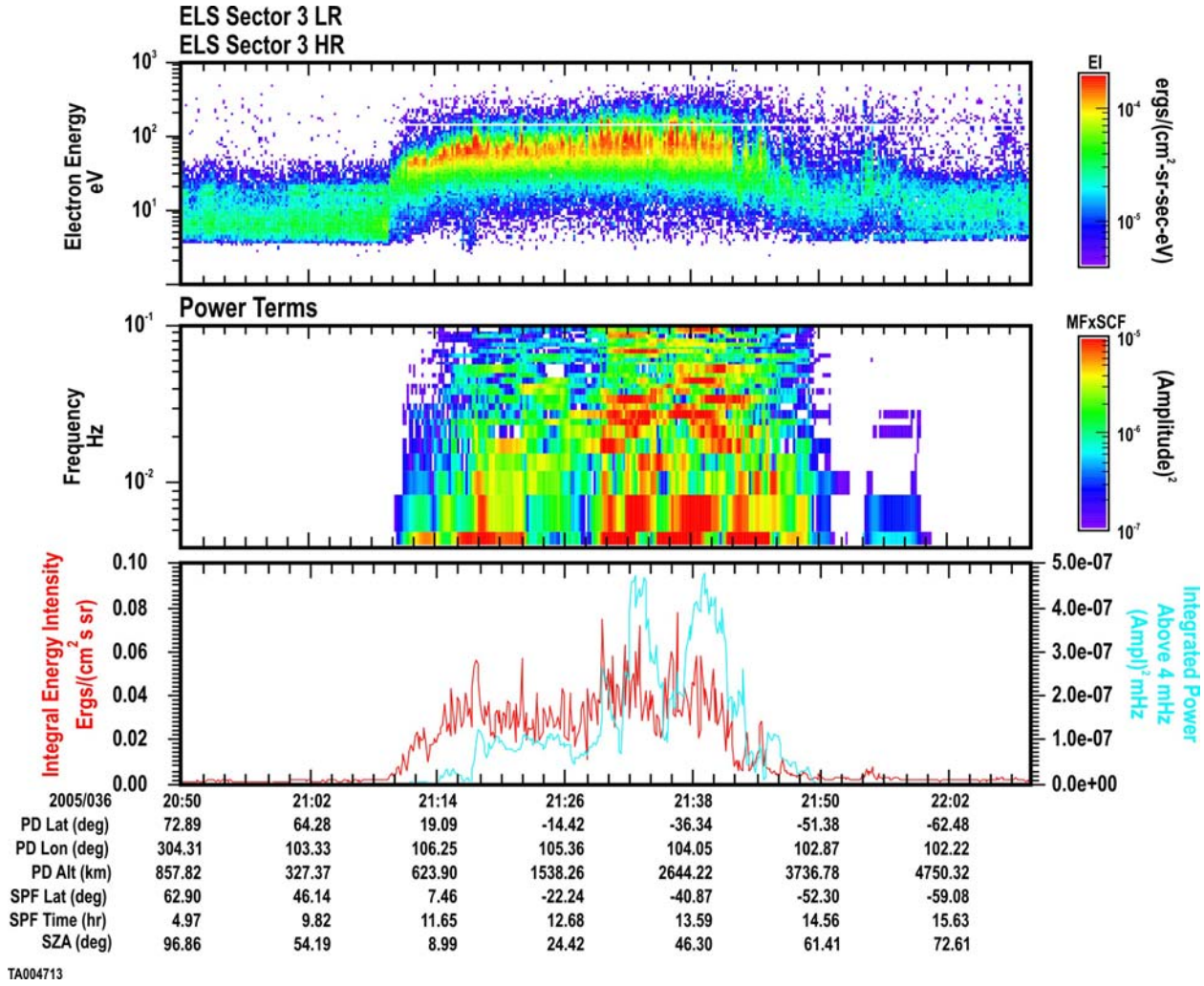
ELS Sector 3 LR
ELS Sector 3 HR
Electron Energy eV
EI
ergs/(cm²-sr-sec-eV)
Power Terms
Frequency Hz
MFxSCF
(Amplitude)²
Integral Energy Intensity Ergs/(cm² s sr)
Integrated Power Above 4 mHz (Ampl)² mHz
2005/036 20:50 21:02 21:14 21:26 21:38 21:50 22:02
PD Lat (deg) 72.89 64.28 19.09 -14.42 -36.34 -51.38 -62.48
PD Lon (deg) 304.31 103.33 106.25 105.36 104.05 102.87 102.22
PD Alt (km) 857.82 327.37 623.90 1538.26 2644.22 3736.78 4750.32
SPF Lat (deg) 62.90 46.14 7.46 -22.24 -40.87 -52.30 -59.08
SPF Time (hr) 4.97 9.82 11.65 12.68 13.59 14.56 15.63
SZA (deg) 96.86 54.19 8.99 24.42 46.30 61.41 72.61
TA004713

Figure 5

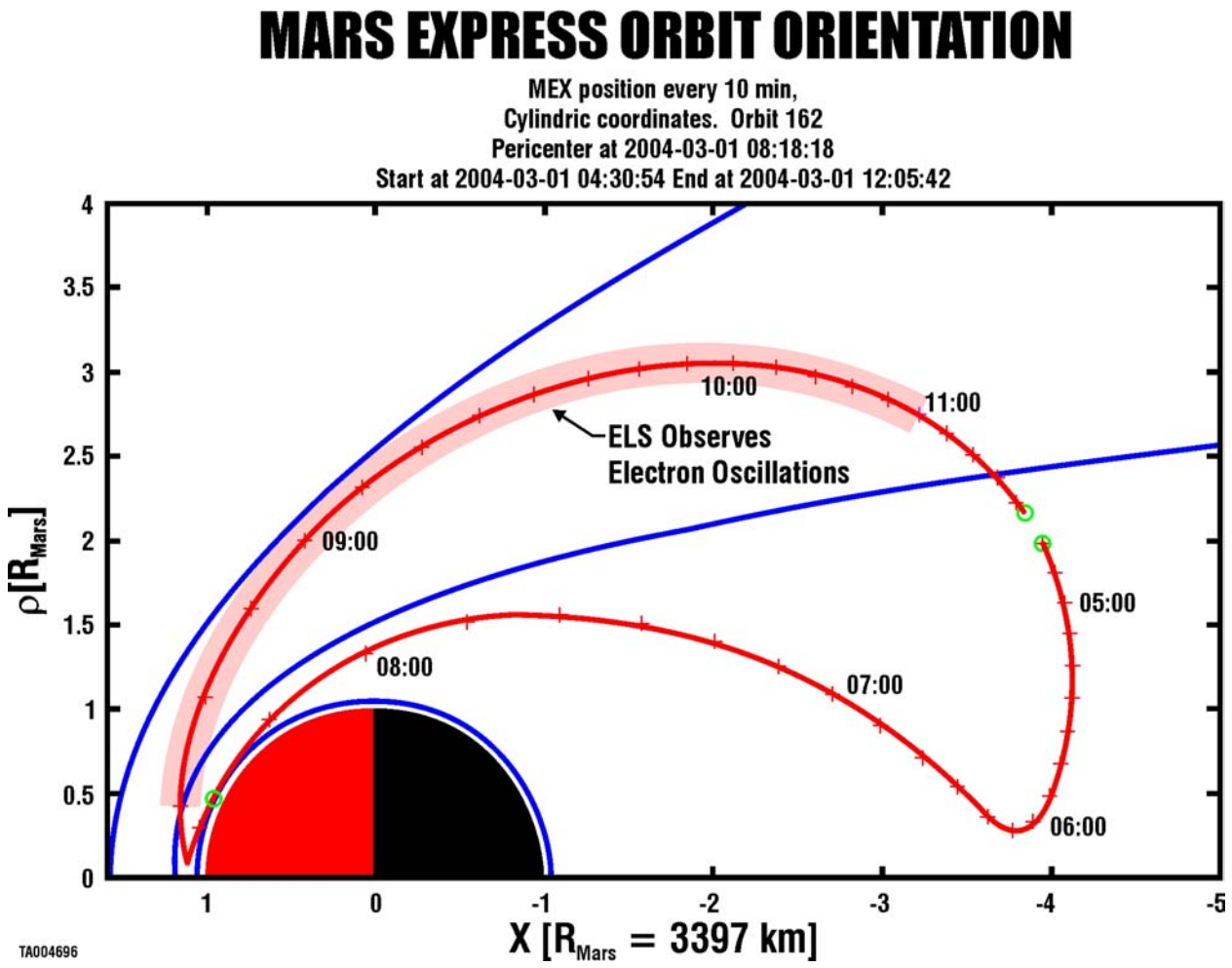
MARS EXPRESS ORBIT ORIENTATION
MEX position every 10 min,
Cylindric coordinates. Orbit 162
Pericenter at 2004-03-01 08:18:18
Start at 2004-03-01 04:30:54 End at 2004-03-01 12:05:42
10:00
11:00
ELS Observes
Electron Oscillations
09:00
05:00
08:00
07:00
06:00
ρ[R_Mars]
X [R_Mars = 3397 km]
TA004696

Figure 6

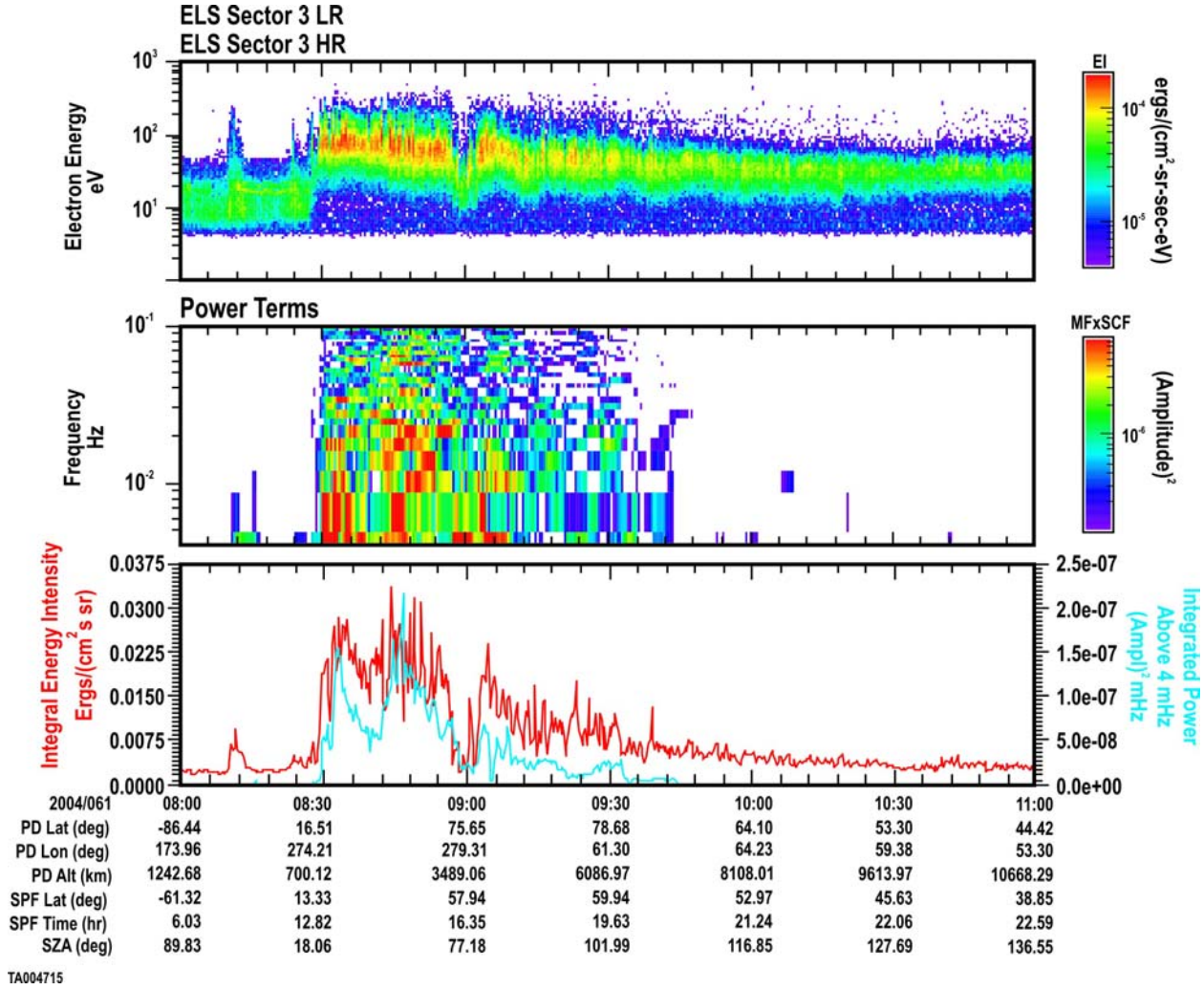
ELS Sector 3 LR
ELS Sector 3 HR
Electron Energy eV
EI
ergs/(cm²-sr-sec-eV)
Power Terms
Frequency Hz
MFxSCF
(Amplitude)²
Integral Energy Intensity Ergs/(cm² s sr)
Integrated Power Above 4 mHz (Ampl)² mHz
2004/061 08:00 08:30 09:00 09:30 10:00 10:30 11:00
PD Lat (deg) -86.44 16.51 75.65 78.68 64.10 53.30 44.42
PD Lon (deg) 173.96 274.21 279.31 61.30 64.23 59.38 53.30
PD Alt (km) 1242.68 700.12 3489.06 6086.97 8108.01 9613.97 10668.29
SPF Lat (deg) -61.32 13.33 57.94 59.94 52.97 45.63 38.85
SPF Time (hr) 6.03 12.82 16.35 19.63 21.24 22.06 22.59
SZA (deg) 89.83 18.06 77.18 101.99 116.85 127.69 136.55
TA004715

Figure 7

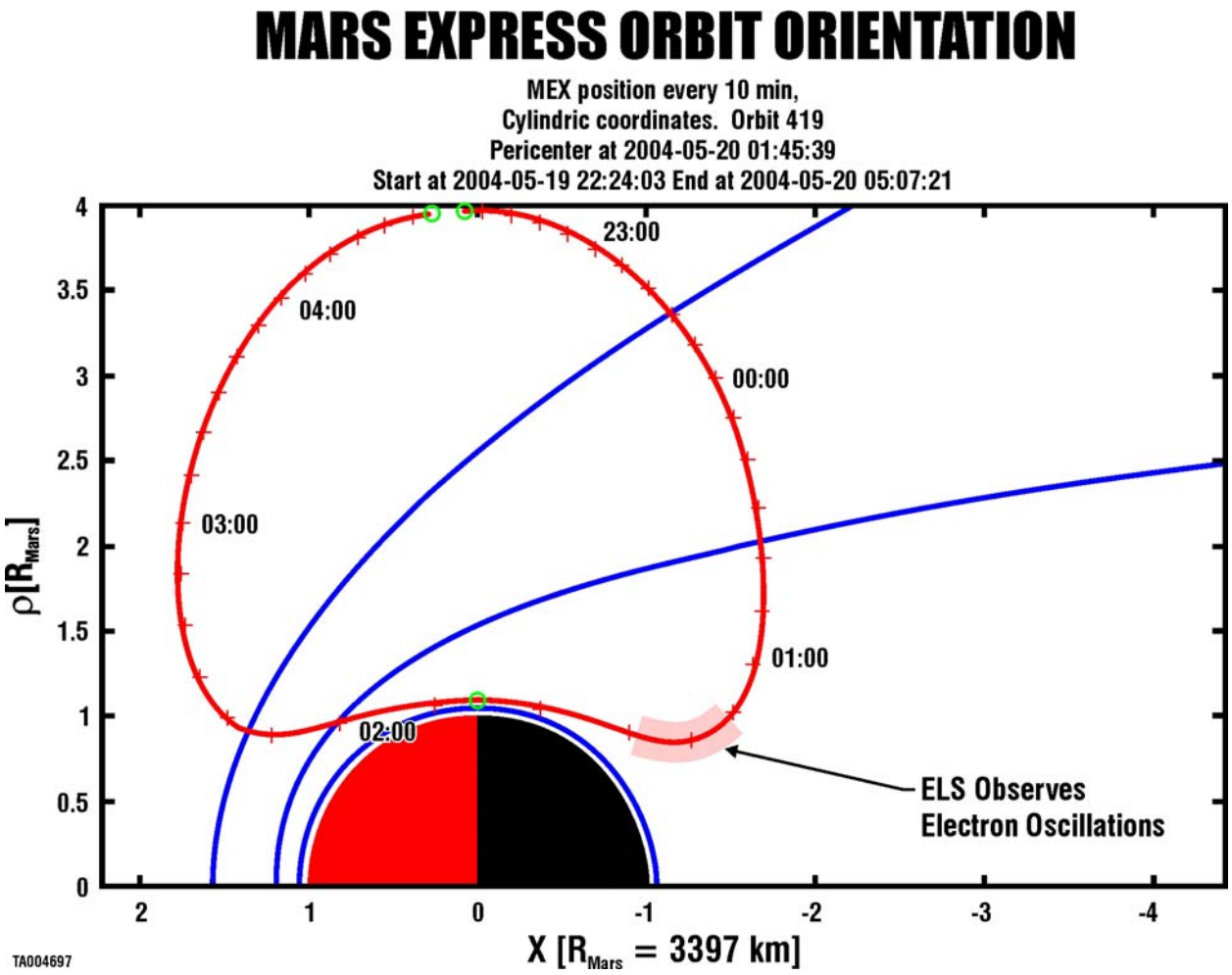
MARS EXPRESS ORBIT ORIENTATION
MEX position every 10 min,
Cylindric coordinates. Orbit 419
Pericenter at 2004-05-20 01:45:39
Start at 2004-05-19 22:24:03 End at 2004-05-20 05:07:21
23:00
04:00
00:00
03:00
01:00
02:00
ELS Observes
Electron Oscillations
ρ[R_Mars]
X [R_Mars = 3397 km]
TA004697

Figure 8

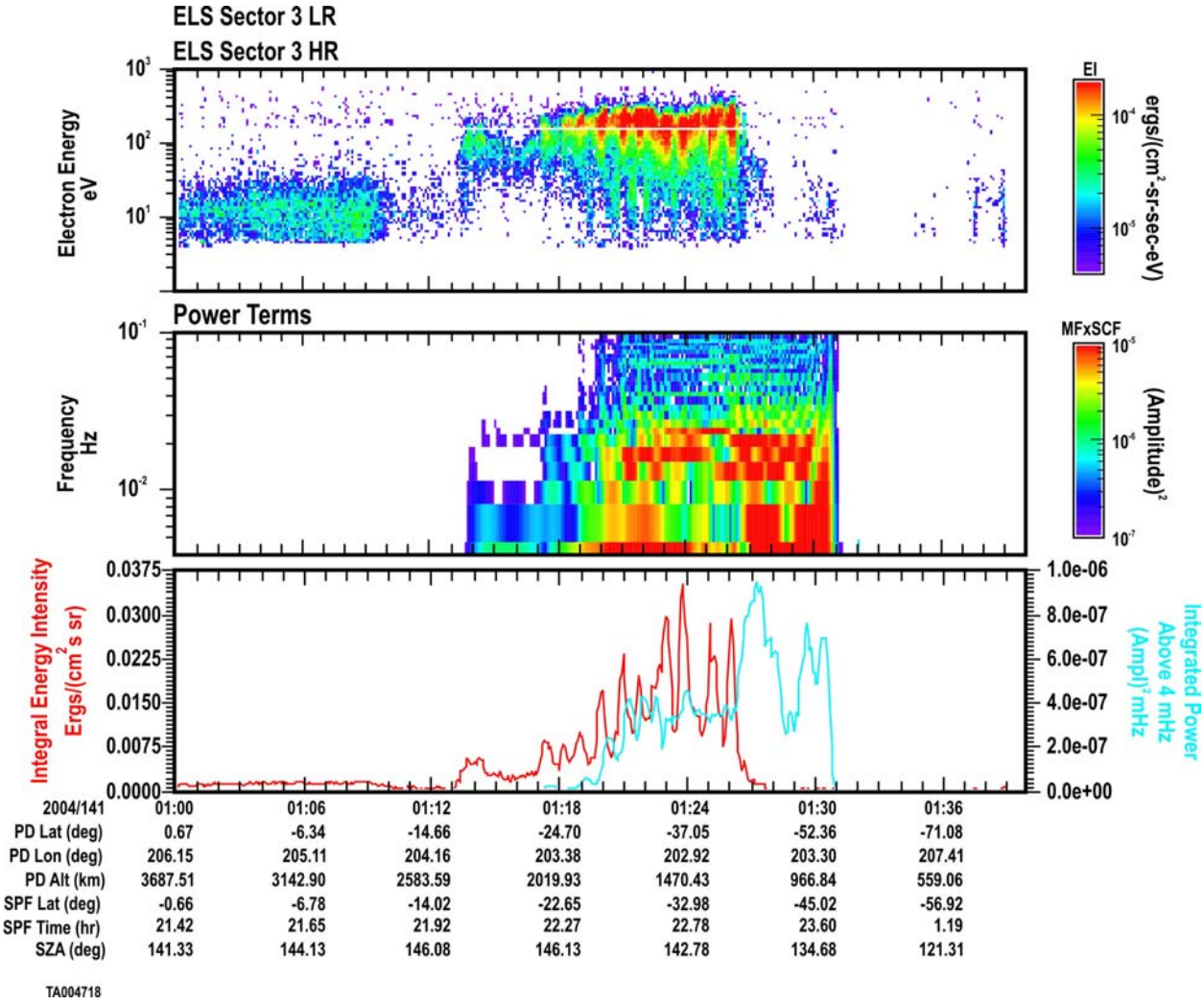
ELS Sector 3 LR
ELS Sector 3 HR
Electron Energy eV
EI
ergs/(cm²-sr-sec-eV)
Power Terms
Frequency Hz
MFxSCF
(Amplitude)²
Integral Energy Intensity Ergs/(cm² s sr)
Integrated Power Above 4 mHz (Ampl)² mHz
2004/141
PD Lat (deg)
PD Lon (deg)
PD Alt (km)
SPF Lat (deg)
SPF Time (hr)
SZA (deg)
TA004718

Figure 9

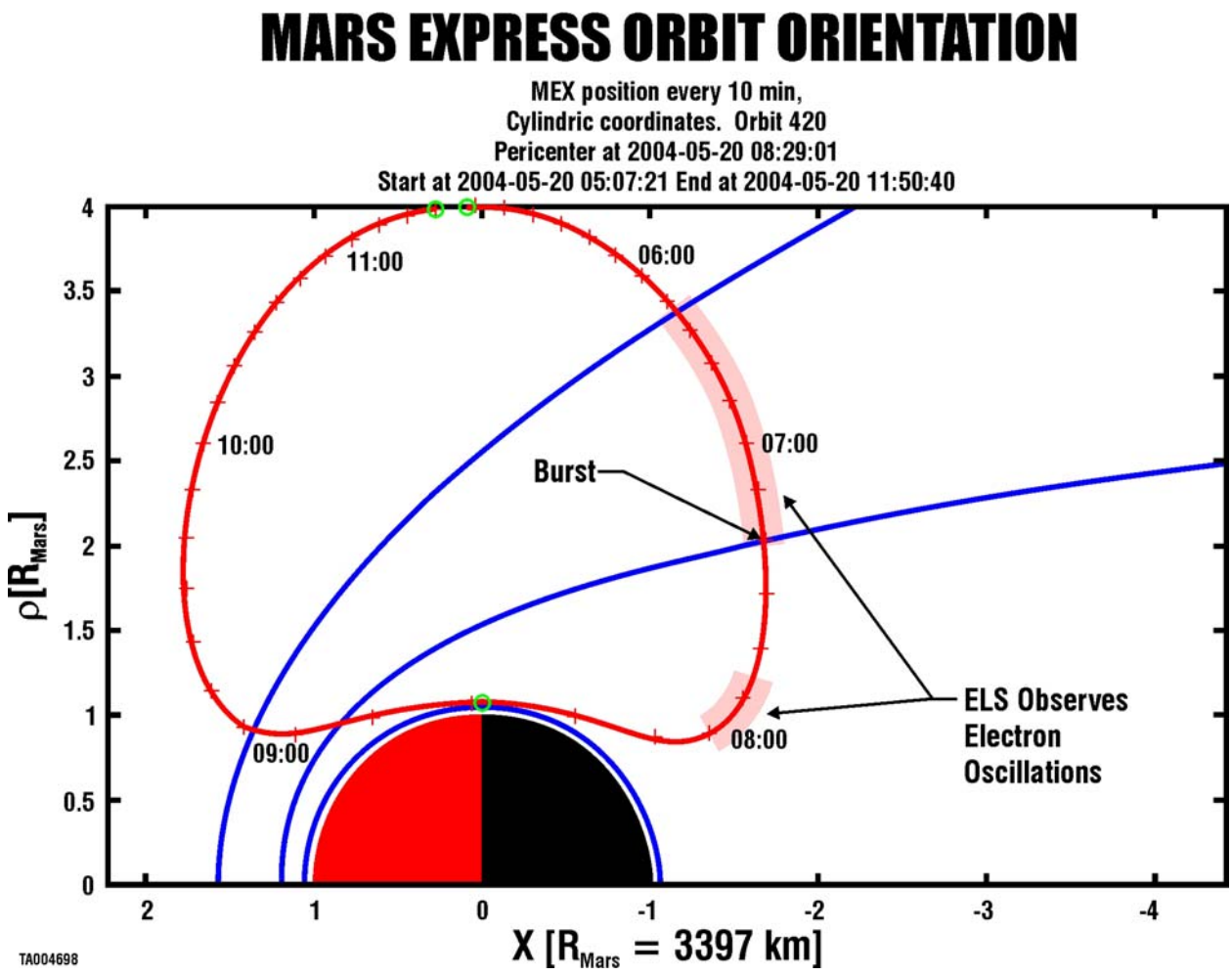
MARS EXPRESS ORBIT ORIENTATION
MEX position every 10 min,
Cylindric coordinates. Orbit 420
Pericenter at 2004-05-20 08:29:01
Start at 2004-05-20 05:07:21 End at 2004-05-20 11:50:40
11:00
06:00
10:00
07:00
Burst
09:00
08:00
ELS Observes
Electron
Oscillations
ρ[R_Mars]
X [R_Mars = 3397 km]
TA004698

Figure 10

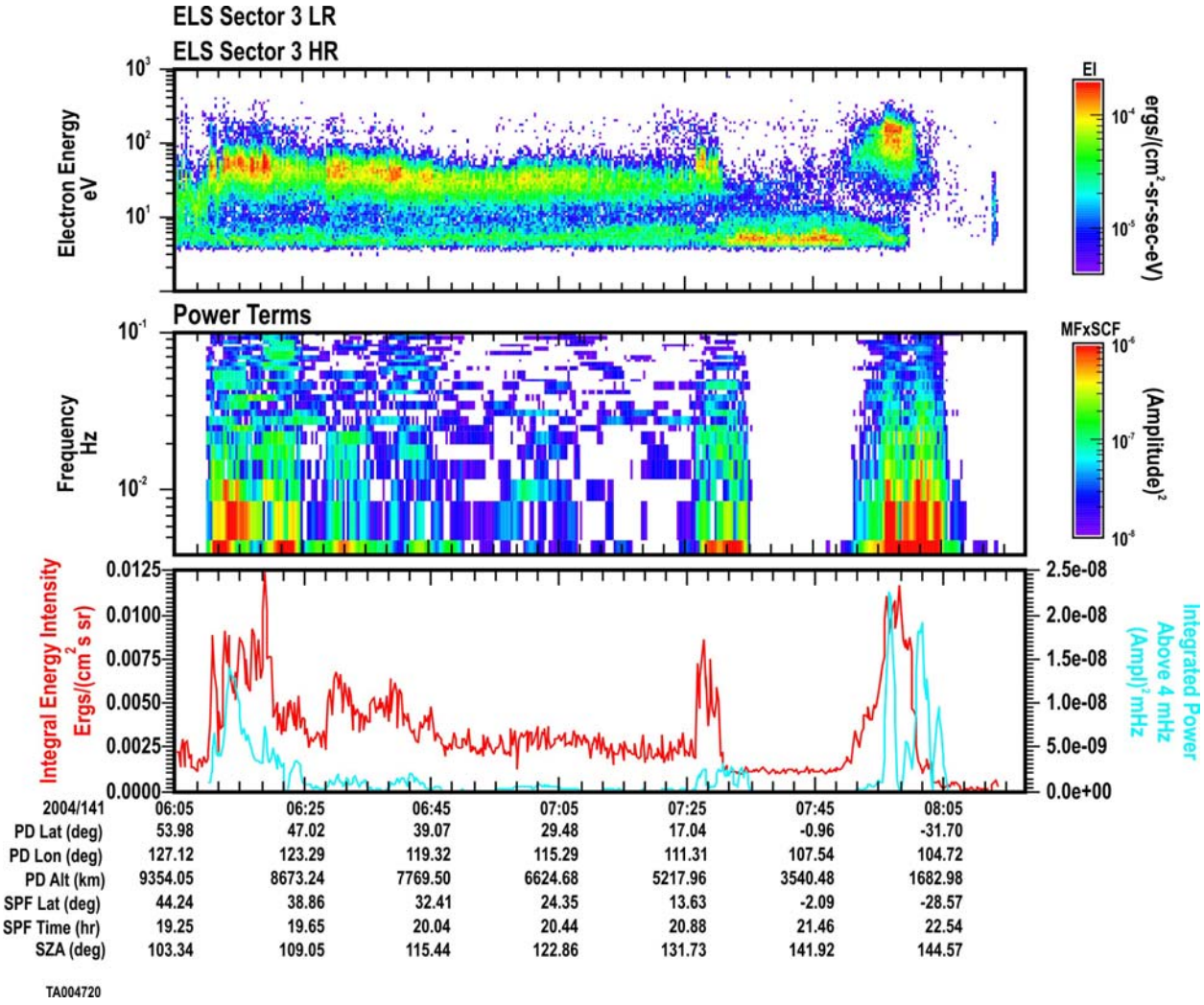
ELS Sector 3 LR
ELS Sector 3 HR
Electron Energy eV
EI
ergs/(cm²-sr-sec-eV)
Power Terms
Frequency Hz
MFxSCF
(Amplitude)²
Integral Energy Intensity Ergs/(cm² s sr)
Integrated Power Above 4 mHz (Ampl)² mHz
2004/141 06:05 06:25 06:45 07:05 07:25 07:45 08:05
PD Lat (deg) 53.98 47.02 39.07 29.48 17.04 -0.96 -31.70
PD Lon (deg) 127.12 123.29 119.32 115.29 111.31 107.54 104.72
PD Alt (km) 9354.05 8673.24 7769.50 6624.68 5217.96 3540.48 1682.98
SPF Lat (deg) 44.24 38.86 32.41 24.35 13.63 -2.09 -28.57
SPF Time (hr) 19.25 19.65 20.04 20.44 20.88 21.46 22.54
SZA (deg) 103.34 109.05 115.44 122.86 131.73 141.92 144.57
TA004720

Figure 11

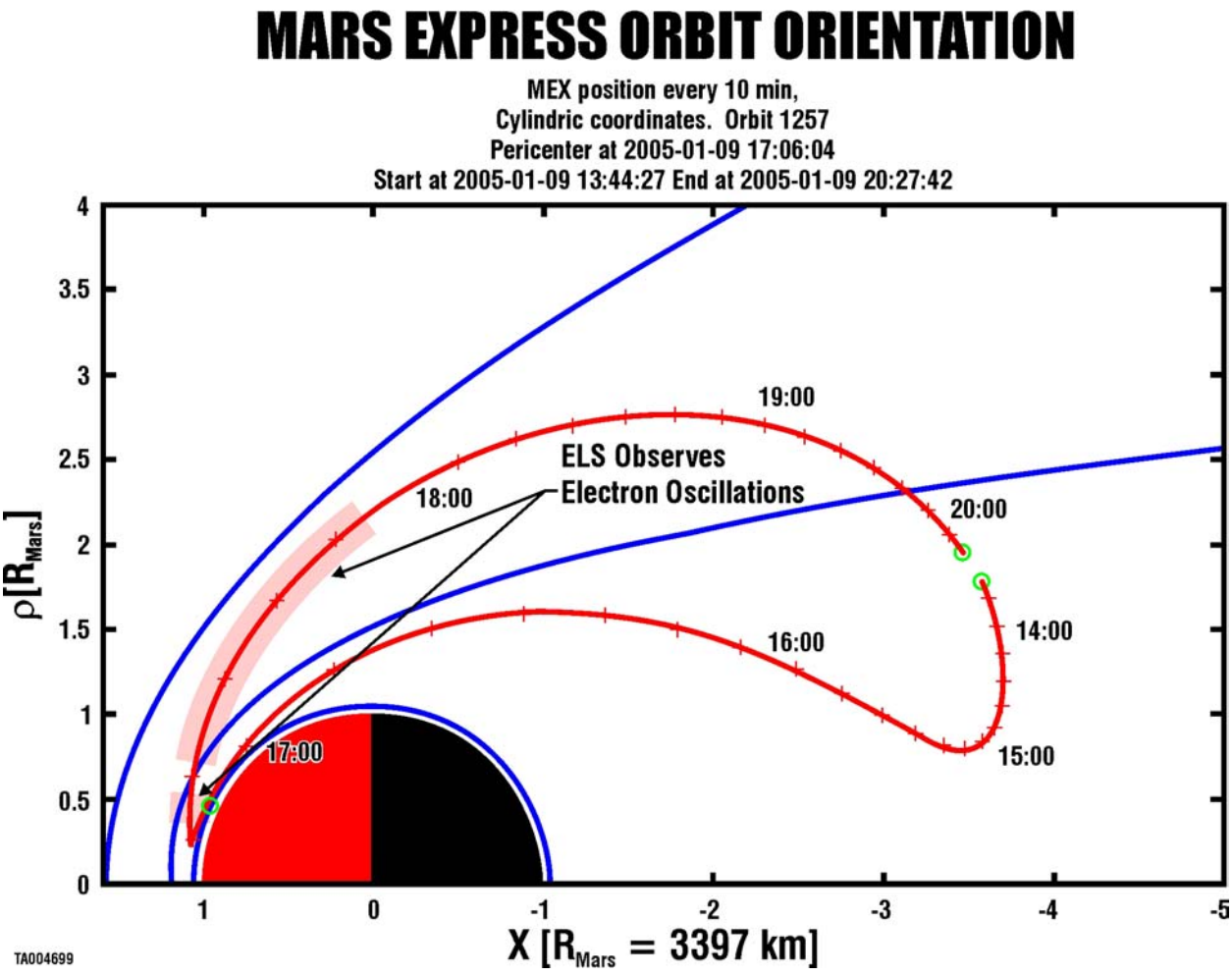
MARS EXPRESS ORBIT ORIENTATION
MEX position every 10 min,
Cylindric coordinates. Orbit 1257
Pericenter at 2005-01-09 17:06:04
Start at 2005-01-09 13:44:27 End at 2005-01-09 20:27:42
ELS Observes
Electron Oscillations
19:00
18:00
20:00
14:00
16:00
17:00
15:00
ρ[R_Mars]
X [R_Mars = 3397 km]
TA004699

Figure 12

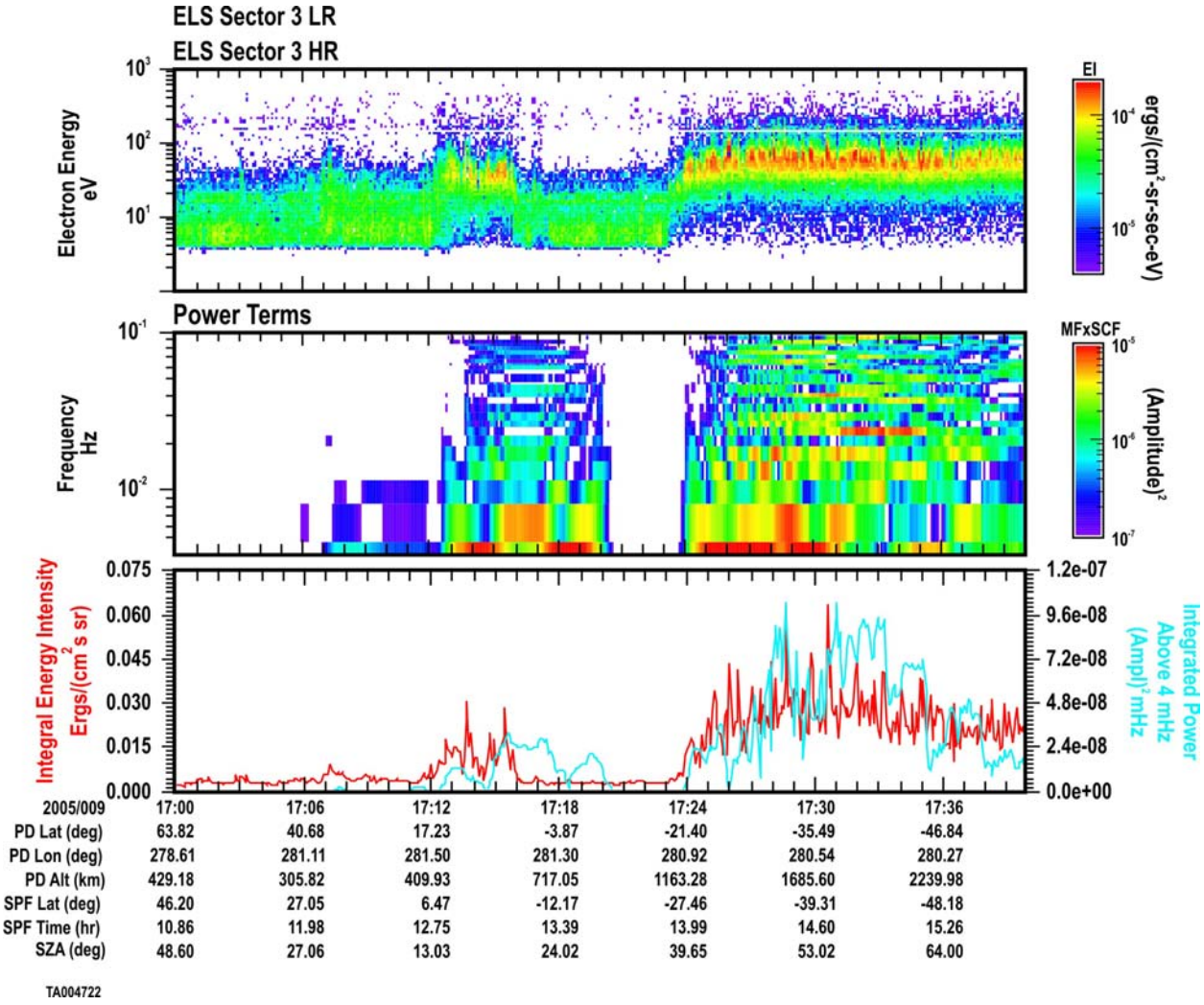
ELS Sector 3 LR
ELS Sector 3 HR
Electron Energy eV
EI
ergs/(cm²-sr-sec-eV)
Power Terms
Frequency Hz
MFxSCF
(Amplitude)²
Integral Energy Intensity Ergs/(cm² s sr)
Integrated Power Above 4 mHz (Ampl)² mHz
2005/009
PD Lat (deg)
PD Lon (deg)
PD Alt (km)
SPF Lat (deg)
SPF Time (hr)
SZA (deg)
17:00 17:06 17:12 17:18 17:24 17:30 17:36
63.82 40.68 17.23 -3.87 -21.40 -35.49 -46.84
278.61 281.11 281.50 281.30 280.92 280.54 280.27
429.18 305.82 409.93 717.05 1163.28 1685.60 2239.98
46.20 27.05 6.47 -12.17 -27.46 -39.31 -48.18
10.86 11.98 12.75 13.39 13.99 14.60 15.26
48.60 27.06 13.03 24.02 39.65 53.02 64.00
TA004722

Figure 13